

TURBULENT TEMPERATURE FLUCTUATIONS IN MERCURY AND ETHYLENE GLYCOL IN PIPE FLOW

J. H. RUST* and ALEXANDER SESONSKÉ

Department of Nuclear Engineering, Purdue University, Lafayette, Indiana

(Received 25 September 1964 and in revised form 31 July 1965)

Abstract—Turbulent temperature fluctuations in mercury and ethylene glycol were measured with a fast response thermocouple having a time constant of the order of 10^{-4} s. Traverses were made across a 0.925 inch diameter horizontal test section having a uniform wall temperature.

Characteristics of the temperature fluctuations measured included the root mean square value, the amplitude distribution, and the frequency distribution, in each case as a function of spatial position and Reynolds number.

The amplitude distribution was found to be non-Gaussian with the deviation greater in mercury. The mean energy of the fluctuations is at frequencies of the order of 8–23 cps.

Thermal mixing lengths compare reasonably well with von Kármán's theoretical mixing lengths. Spectral density results only partially follow Corrsin's frequency dependence.

NOMENCLATURE

f ,	frequency [cps];
$G(f)$,	"time" spectrum of temperature fluctuations;
$G(k)$,	"spatial" spectrum of temperature fluctuations;
k ,	wave number;
l_t ,	thermal mixing length;
l_u ,	velocity mixing length;
L ,	length scale of large eddies;
N_{Re} ,	Reynolds number;
N_{Pr} ,	Prandtl number;
$P(x)$,	probability density function;
$P(X)$,	cumulative probability distribution function;
r ,	radial distance variable;
r_o ,	tube radius;
$\sqrt{\overline{t'^2}}$,	root-mean-square temperature fluctuations [degF];
$\overline{t'^2}$,	mean square of temperature fluctuations [degF ²];
\overline{T} ,	mean temperature [°F];
T_{min} ,	minimum fluid temperature [°F];
T_w ,	wall temperature [°F];
U' ,	r.m.s. of velocity fluctuations;
u ,	fluid velocity;

α ,	thermal diffusivity;
ϵ ,	total rate of viscous dissipation of kinetic energy per unit mass of fluid;
ν ,	kinematic viscosity.

INTRODUCTION

ALTHOUGH liquid metal heat-transfer rates in turbulent flowing systems may be described by integral equations of various types which make use of the eddy diffusivity approach, the use of profile methods to experimentally confirm the models involved has been difficult and only partially successful [1]. Since such thermal transport is actually a result of turbulent exchange processes, a theoretical and experimental study of turbulent heat transfer from the stochastic viewpoint provides insight into mechanisms and could lead to a consistent theory applicable to both metals and non-metals. As a first step, therefore, a study was made of the turbulent temperature fluctuations occurring in two different fluids, mercury and ethylene glycol, in pipe flow.

Little has been published on the application of statistical methods to turbulent heat transfer. Corrsin [2, 3] treated the decay of isotropic temperature fluctuations in isotropic flow and also developed expressions for the spectrum of isotropic temperature fluctuations.

* J. H. Rust is with the Nuclear Engineering Department, University of Virginia, Charlottesville, Virginia.

The spectrum of temperature fluctuations was analysed in more detail by Batchelor [4] for fluids of $N_{Pr} \gg 1$ and by Batchelor, Howells and Townsend [5] for fluids of $N_{Pr} \ll 1$, with the result that expressions were developed for the temperature spectrum which cover a wider range of wave numbers than the expression proposed by Corrsin.

By use of Onsager's cascade model for turbulent spectra, Corrsin [6] recently determined expressions for the temperature spectrum which differ from those previously reported.

Experimental measurements of turbulent temperature fluctuations have been rather limited. Corrsin measured various statistical properties of temperature fluctuations in air in the wake of a heated jet [7] and behind a heated grid [8]. Subbotin [9, 10] investigated temperature fluctuations in water and in a liquid metal in pipe flow. Johnson [11] measured simultaneous velocity and temperature fluctuations in the thermal boundary layer along a heated flat plate. Tanimoto and Hanratty [12] as well as Rodriguez-Ramirez [13] studied temperature fluctuations in an air system.

In the present investigation, measurements were performed in a low Prandtl number fluid, mercury ($N_{Pr} \approx 0.018$) and a high Prandtl

number fluid, ethylene glycol ($N_{Pr} \approx 44$) in order to compare results in two classes of heat-transfer media. Parameters studied were mean-temperature distributions and the following properties of the temperature fluctuations: time-average root-mean-square, amplitude distribution, and spectrum. These properties were studied under uniform wall-temperature boundary conditions at different Reynolds numbers, spatial positions, and heat fluxes.

DESCRIPTION OF EQUIPMENT

The heat-transfer loop (Fig. 1), constructed of $\frac{3}{4}$ inch, sch. 5, type 304 stainless tubing, included a 4.0 ft long, horizontal test section 0.925 in ID preceded by a straight 6.0 ft length of tubing corresponding to an L/D ratio of 78. A centrifugal pump was used for circulation.

The temperature probe (Fig. 2), could be moved in two-dimensions through the use of a ball-joint assembly sealed from the working fluid by a stainless steel bellows. Probe movement was measured by a dial gage sensitive to 0.0005 in. The probe tip was located 46 in from the test section entrance to provide an L/D ratio of 50 which was beyond that predicted by Sleicher and Tribus [14] in order to be in the asymptotic Nusselt number region for liquid

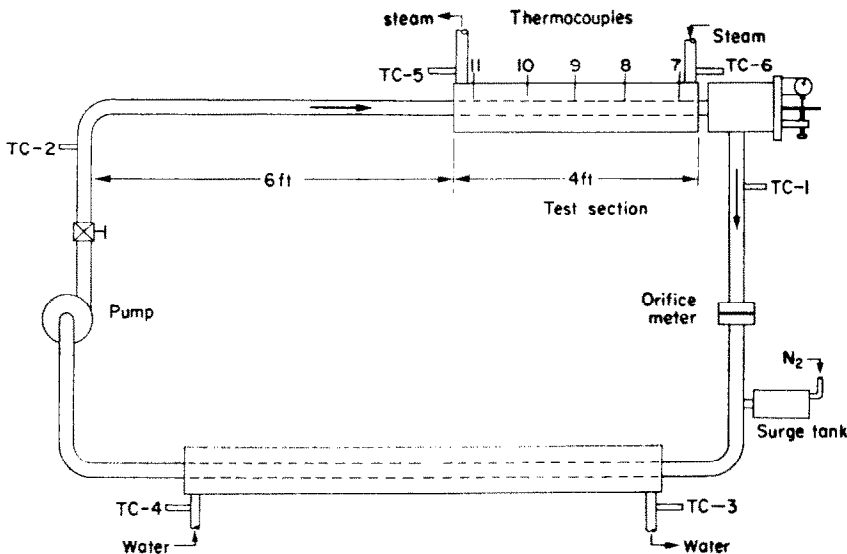


FIG. 1. Heat-transfer loop.

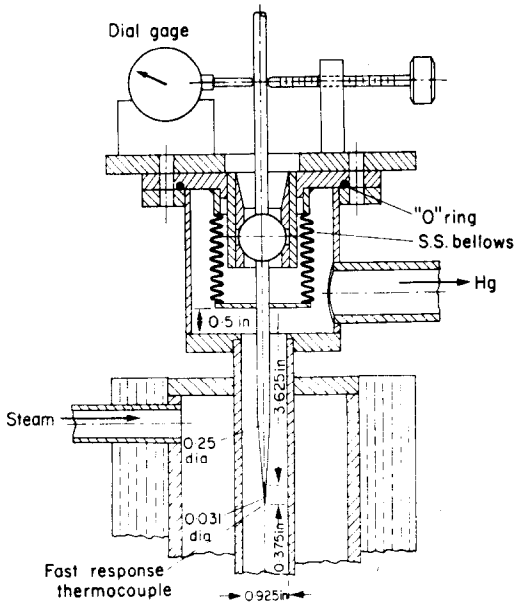


FIG. 2. Temperature probe.

metals under uniform wall-temperature conditions.

The fast response thermocouple, supplied by Mo'Re of Bonner Springs, Kansas, was fabricated from an oxide-coated constantan wire around which was swaged a Chromel tube to a

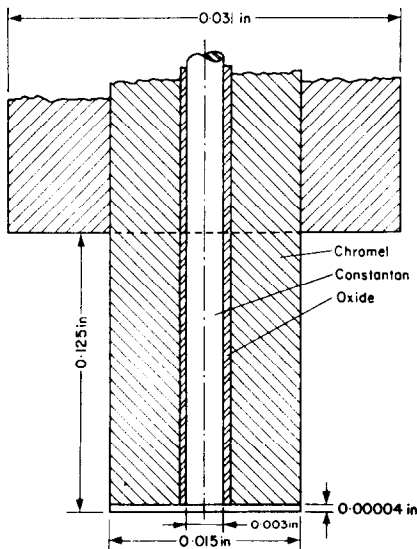


FIG. 3. Fast response thermocouple.

final diameter of 0.015 in. The thermocouple junction was made by vacuum depositing a thin nickel plate on a metallurgically polished end of the wire-tube assembly. This design results in a thermocouple time constant estimated to be of the order of 10^{-4} s [15]. The frequency response of the thermocouple should therefore be essentially flat up to frequencies of the order of 1000 cps.

Condensing steam was used for heating the test section to minimize electrical noise. Variable wall temperatures were possible by changing the steam pressure.

INSTRUMENTATION

The direct component of the thermocouple signal was measured by a Rubicon Potentiometer capable of detecting signal differences to 10^{-7} V. A Tektronix 122, low level pre-amplifier, used as shown in Fig. 4, was modified to increase its effective gain to 3600 and reduce its inherent noise level to $0.55 \mu\text{V}$ (r.m.s.) [15]. By use of the differential input of the amplifier and proper noise control techniques, the noise level of the entire system was reduced to less than $0.60 \mu\text{V}$ (r.m.s.), negligible in comparison to the desired signals which were of the order of 20–300 μV .

The amplified signal from the thermocouple was fed into various recording instruments, Fig. 4, designed to analyse random signals. A Ballantine Model 320A True Root-Mean-Square Electronic Voltmeter was used for r.m.s. measurements of the fluctuating signal. The frequency response of the combined amplifier and r.m.s. voltmeter was relatively flat from 2 to 600 cps. Since the "energy" of the temperature fluctuations at frequencies above 600 cps was negligible, all loss of information in the r.m.s. measurements was due to the low frequency cut-off of the combined system. It is estimated that the low frequency cut-off contributed less than a 5 per cent error in r.m.s. measurements of the fluctuating signal. The r.m.s. voltmeter was modified to increase its averaging time for random signals by inserting a 500 Ω resistor in series and a 10 000 μf capacitor in parallel with the voltmeter's indicator galvanometer terminals. Frequency analysis was accomplished with a General Radio Model 262 Vibration Analyzer. Since this instrument would overload at low frequencies when the input signal was above the

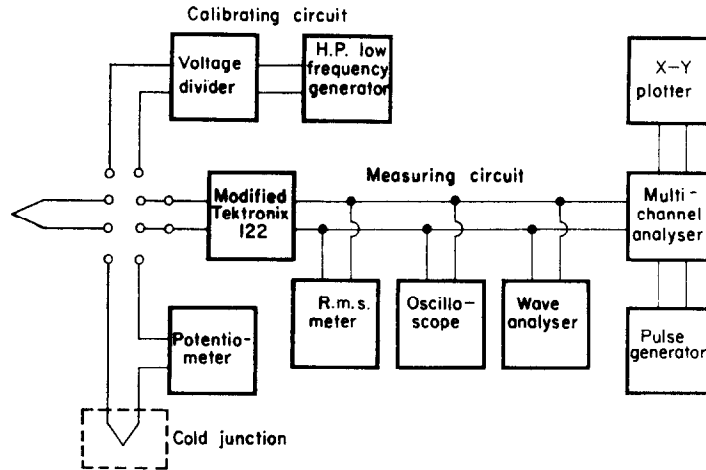


FIG. 4. Block diagram of electronic circuits.

millivolt range, low frequency data would be considered semi-quantitative. A RIDL Model 34-12, 400 channel pulse height analyser was used to determine the probability density function of the temperature fluctuations. A gating circuit built into the analyser digitalized the random signal from the amplifier into pulses of less than $14 \mu\text{s}$ duration at the rate of 1000 samples/s. The instrument was then used as a digital voltmeter with a built-in computer to analyze the amplitudes of the digitalized data (see reference [15] for details of operations).

EXPERIMENTAL RESULTS

Measurements were made at the conditions shown in the Table 1.

For the measurements in mercury, the symbols *A* and *B* serve to indicate conditions of high average heat flux *A* and reduced average heat flux *B*.

Mean temperature

Figures 5 and 6 illustrate mean-temperature distributions for mercury and ethylene glycol, respectively, at the conditions given in Table 1. The ordinate, a normalized temperature, is defined by $(T_w - \bar{T}) / (T_w - \bar{T}_{\min})$ where T_w is the wall temperature and \bar{T}_{\min} is the minimum fluid temperature found in the traverses across the tube diameter. The abscissa is a normalized radius in which r is the distance from the tube center and r_o is the tube radius ($r/r_o = -1$

Table 1. Experimental conditions

	Steam Temp. (°F)	Flow Rate (lb/h)	N_{Re}	T_{in} (°F)	T_{out} (°F)	$\overline{Q/A}$ (Btu/h ft ²)
Mercury (<i>A</i>)	246	8660	49 500	118	213	32 000
Mercury (<i>A</i>)	246	26 400	145 500	145	195	40 200
Mercury (<i>A</i>)	245	42 700	236 000	160	192	42 400
Mercury (<i>B</i>)	212	26 750	143 000	137	172	33 300
Mercury (<i>B</i>)	211	46 000	243 000	140	169	35 800
Glycol	253	3560	5800	156	164	17 600
Glycol	250	6820	12 600	166	172	26 200

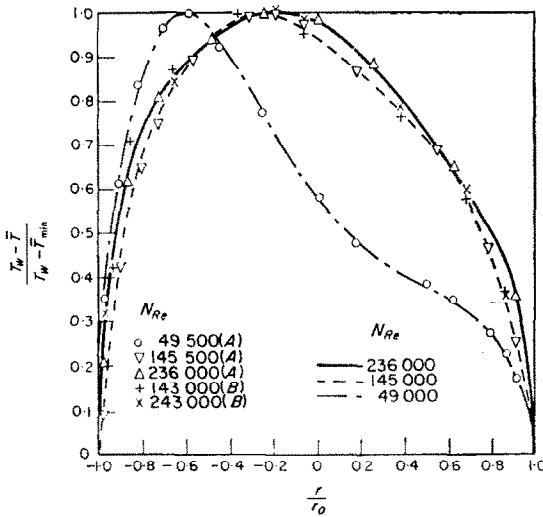


FIG. 5. Mean temperature distribution in mercury for different Reynolds numbers.

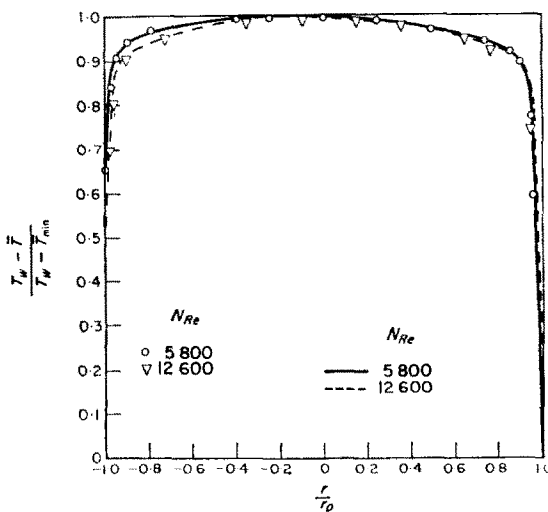


FIG. 6. Mean temperature distribution in glycol for different Reynolds numbers.

corresponds to the bottom tube wall). The curves in Figs. 5 and 6 represent a least square fit of the actual experimental data to a fifth order power series.

The mean-temperature distributions in mercury are asymmetric, with minimum fluid temperatures displaced toward the bottom tube wall instead of at the center (Fig. 5). Two

explanations for this behavior are possible: (1) uniform-wall temperature conditions might not exist because of the angularly dependent condensing steam heat-transfer coefficient, and (2) free convection might occur perpendicular to the mean flow. Both of these factors are thought to be responsible for the asymmetry of the mercury temperature profiles. Similar natural convection asymmetry has been reported by Buyco [16] for mercury and Schrock [17] for NaK flow in horizontal tubes with constant-wall heat-flux boundary conditions.

The mean-temperature distributions in ethylene glycol (Fig. 6) also exhibit asymmetry, although the distortion is slight compared to that in mercury. Non-uniformity in wall temperature may explain this behavior.

R.m.s. temperatures

Distributions of the root-mean-square of the temperature fluctuations are shown in Fig. 7 for mercury at the conditions given in Table 1. As shown, the r.m.s. temperatures are asymmetric with respect to the tube axis, probably due to free convection and non-uniform wall temperatures. The mercury r.m.s. temperatures reach a maximum near the tube wall, at approximate values of $|r/r_0| = 0.8-0.9$. From the maximum

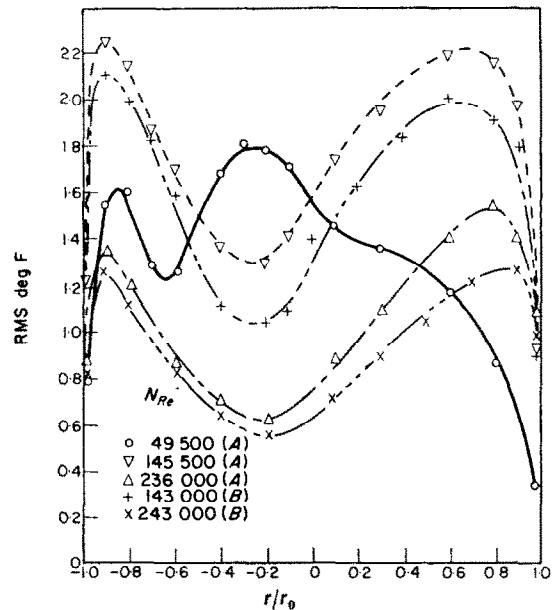


FIG. 7. R.m.s. temperature fluctuations in mercury.

value, there is a gradual decrease toward the tube axis and a sharp decrease toward the tube wall. These results are somewhat in disagreement with measurements of Subbotin [9] who has reported maximum r.m.s. temperatures in liquid metals to be halfway between the tube wall and axis, or $|r/r_o| = 0.5$. In Subbotin's case, however, free convection was negligible.

The dependence of r.m.s. temperatures on Reynolds number is somewhat obscure. As Fig. 7 illustrates, the magnitude increases as the Reynolds number increases from 49 500 to 145 500 and then decreases as the Reynolds number increases from 145 500 to 243 000. This is contrary to the measurements of Subbotin [10] who reported r.m.s. temperatures in liquid metals to be a decreasing function of Reynolds number with maximum values occurring near the critical Reynolds number for turbulent flow (N_{Re} equal to 2300).

The r.m.s. data shown in Fig. 7 are presented on a non-normalized basis to avoid introducing the effect of uncertainties in wall temperature or other parameters which could serve as the basis for normalization.

R.m.s. temperatures are dependent upon the wall heat flux. Increasing the heat flux produces an increase in the magnitude of the fluctuations (A indicates the higher heat flux) but essentially produces no change in the spatial distribution. This may be explained by r.m.s. temperatures being dependent upon the local mean-temperature gradient, since increasing the heat flux produces larger temperature gradients within the fluid. By comparing mean temperatures (Fig. 5) with r.m.s. temperatures (Fig. 7), it is seen that in a direction away from the tube wall, minimum r.m.s. temperatures occur at the position of minimum fluid temperature or zero mean-temperature gradient. A more detailed discussion of this effect appears later in this section.

Figure 8 illustrates ethylene glycol r.m.s.-temperature distributions. The distributions are almost symmetric with respect to the tube axis with the slight amount of asymmetry at a Reynolds number of 12 600 probably due to a non-uniform wall temperature. Once again the r.m.s. temperatures were not normalized because of the uncertainty in the values of the normalizing parameters.

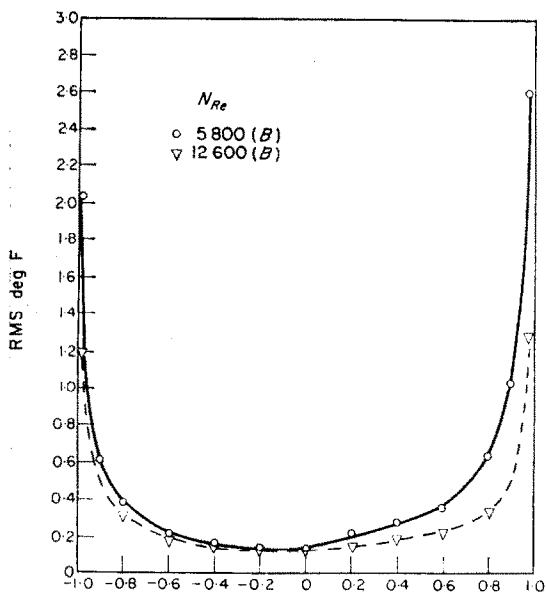


FIG. 8. R.M.S. temperature fluctuations in ethylene glycol.

The spatial dependence of r.m.s. temperatures in ethylene glycol differs considerably from the dependence shown in mercury (Fig. 7). Maximum r.m.s. temperatures occur at a position corresponding to the probe touching the tube wall. From the maximum, the r.m.s. temperatures decrease sharply to an approximate position of $|r/r_o| = 0.9$ and then decrease gradually to a minimum value near the tube axis. Similar behavior was reported by Subbotin for r.m.s. measurements in water [10]. The occurrence of maximum r.m.s. temperatures very near the wall may be due to the influence of the local mean-temperature gradient on the fluctuations. As seen by comparing Figs. 5 and 6, in the vicinity of the wall the ethylene glycol temperature gradients are several orders of magnitude higher than the corresponding liquid metal gradients.

Under turbulent flow conditions, temperature fluctuations were observed in both mercury and ethylene glycol when the temperature probe touched the tube wall. Since the probe diameter (0.015 in) exceeded computed thicknesses of the laminar sublayer, the measurements were not conclusive regarding the existence of such a layer. However, if the probe would have

been small enough to penetrate the laminar sublayer, some temperature fluctuations would be expected, since thermocouples mounted on the outside of the test section indicated temperature fluctuations in the wall.

From experimental mean and r.m.s. temperatures it is possible to compute a thermal mixing length as defined by the relation,

$$\bar{l} = l_t \left| \frac{dT}{dr} \right|, \quad (1)$$

where \bar{l} is the r.m.s. temperature, l_t the thermal mixing length, and dT/dr the mean-temperature gradient. This is analogous to the mixing lengths defined by Prandtl to characterize velocity fluctuations.

$$\bar{u}' = l_u \left| \frac{dU}{dr} \right| \quad (2)$$

Equation (1) is rearranged to make it more suitable for the calculation of thermal mixing lengths,

$$\frac{l_t}{r_o} = \frac{\bar{l}}{\left| dT/d(r/r_o) \right|}. \quad (3)$$

Since determining temperature gradients by graphical differentiation of experimental curves is subject to serious errors, a least square method was used to fit differentiable equations to the mean-temperature data and $\left| dT/d(r/r_o) \right|$ was computed from these equations.

In spite of precautions taken, the accurate determination of temperature gradients near the wall in ethylene glycol was virtually impossible since temperature gradients ranged from 6000 to 35 000 degF/ft. Consequently for $|r/r_o|$ greater than 0.9, the thermal mixing lengths should be regarded as indicating only qualitative trends. For mercury, the temperature gradients near the wall are not as severe and, consequently, the computed temperature gradients near the wall are considered much more reliable.

The experimental thermal mixing lengths in mercury and ethylene glycol, Fig. 9, show a close

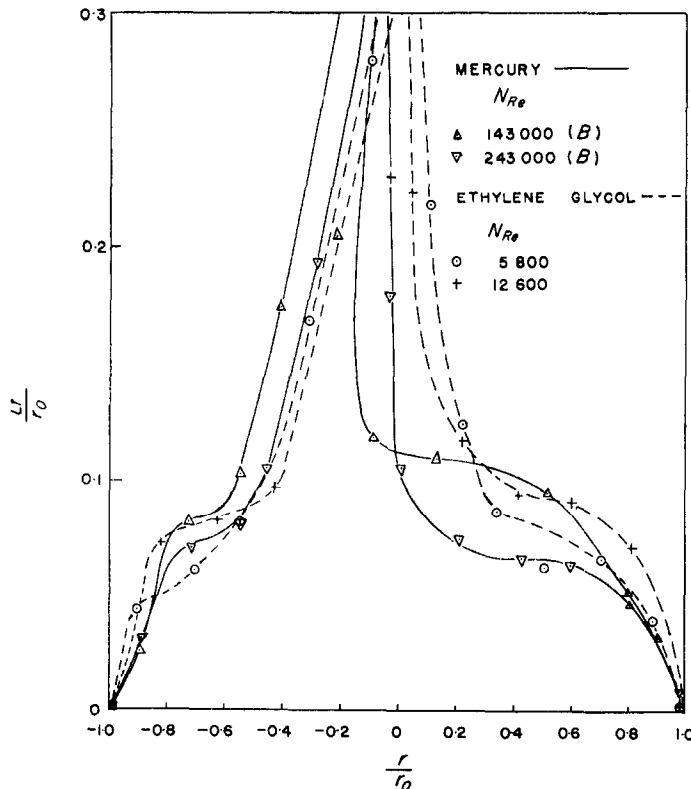


FIG. 9. Thermal mixing length for mercury and ethylene glycol.

similarity. This relative agreement over a wide range of flow conditions for two vastly different fluids indicates that a general relationship may exist between r.m.s. temperatures and local mean-temperature gradients. Although spatial distribution of r.m.s. temperatures in mercury and ethylene glycol are different, ethylene glycol has maximum values at the wall (Fig. 8) while mercury has maximum values displaced away from the wall (Fig. 7), the relationship between r.m.s. temperatures and local mean-temperature gradients is similar.

The velocity mixing length expressions taken from experimental data have been shown to be independent of Reynolds number, i.e. Nikuradse's [21] expression computed from his velocity measurements. A general lack of sensitivity to Reynolds number is also apparent in the case of the experimental thermal mixing lengths determined in this investigation. Furthermore, the qualitative agreement between experimental thermal mixing lengths and the predictions of various velocity mixing length theories suggests that additional experimental work may be helpful in resolving some of the uncertainties in mixing length models used in the development of heat-transfer integral equations.

Spectrum

In the inertial subrange, the spectrum of velocity fluctuations shows the wave-number dependence

$$F(k) \sim k^{-5/3} \tag{4}$$

The lower wave-number cut-off for the range of validity of equation (4) is for $k \gg L^{-1}$ where L is the length scale of the larger eddies. The upper wave-number cut-off of the inertial subrange due to viscous effects is near $(\epsilon/\nu^3)^{1/4}$.

Batchelor [4, 5] and Corrsin [3] assumed that the hypotheses of Kolmogoroff's universal equilibrium theory can be applied to temperature fields as well as velocity fields. It therefore follows that there exists a range of wave-numbers in which molecular conduction is unimportant, termed the convection subrange.

For fluids with $N_{Pr} \gg 1$, the convection subrange extends to higher wave-numbers than the inertial subrange. The upper wave-number conduction cut-off is near $(\epsilon/\nu\alpha^2)^{1/4}$. For large Prandtl number fluids, Batchelor [4] and Corrsin

[3] showed that within the inertial subrange the spectrum of temperature fluctuations will have the same wave-number dependence as the spectrum of velocity fluctuations provided that the statistical properties of the small-scale components of the temperature field are homogeneous, isotropic, and steady. For higher wave-numbers beyond those corresponding to the inertial subrange, Batchelor proposed that the temperature spectrum is proportional to k^{-1} . In summary, the temperature spectrum for fluids with $N_{Pr} \gg 1$ is given by

$$G(k) \sim k^{-5/3} \tag{5}$$

for $L^{-1} \ll k \ll (\epsilon/\nu^3)^{1/4}$

and

$$G(k) \sim k^{-1} \tag{6}$$

for $(\epsilon/\nu^3)^{1/4} \ll k \ll (\epsilon/\nu\alpha^2)^{1/4}$.

For fluids with $N_{Pr} \ll 1$, the conduction cut-off for the temperature spectrum occurs within

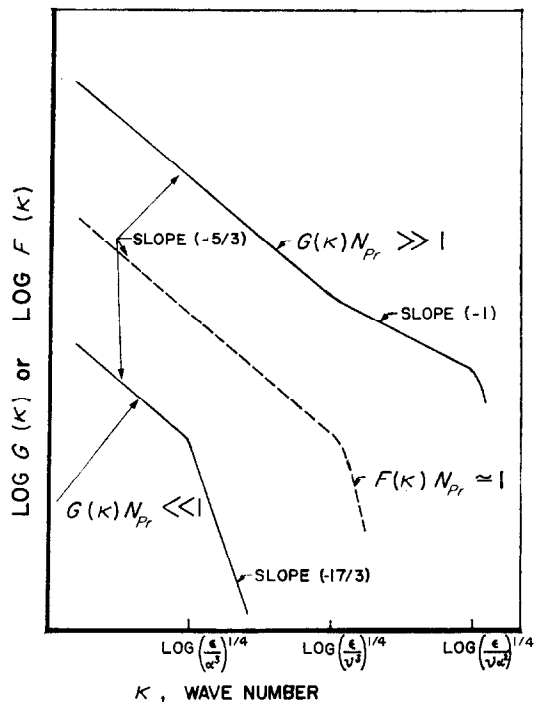


FIG. 10. Theoretical spectra for velocity and temperature fluctuations,

the inertial subrange. Batchelor, Townsend and Howells [5] proposed the conduction cut-off to be near $(\epsilon/\alpha^3)^{1/4}$. Within the inertial subrange and at wave-numbers below the conduction cut-off, the temperature spectrum still has the $k^{-5/3}$ dependence. However, for wave-numbers above the conduction cut-off and less than the viscous cut-off, the proposed wave-number dependence is $k^{-17/3}$. Therefore, for fluids with $N_{Pr} \gg 1$, the temperature spectrum in the inertial-convective subrange is given by

$$G(k) \sim k^{-5/3} \tag{7}$$

where $L^{-1} \ll k \ll (\epsilon/\alpha^3)^{1/4}$ and for the inertial-diffusive subrange by

$$G(k) \sim k^{-17/3} \tag{8}$$

where $(\epsilon/\alpha^3)^{1/4} \ll k \ll (\epsilon/\nu^3)^{1/4}$.

Figure 10 illustrates this theoretical wave-numbers dependence of the temperature spectrum for the two classes of fluids.

Very few data are available on the measurement of the spectra of convected quantities in turbulent flow. Corrsin [7] showed a $k^{-5/3}$ dependence for the spectrum of temperature fluctuations in the wake of a heated jet. Gibson and Schwarz [18] measured the spectrum of concentration fluctuations of salt water ($N_{Sc} \gg 1$) in turbulent flow behind a grid. Their data showed agreement with Batchelor's spectral theory for the inertial-convective subrange and the viscous-convective subrange.

In Taylor's hypothesis, frequency is related to wave-numbers by

$$k = \frac{2\pi f}{U} \tag{9}$$

where U is the local mean velocity. This relation is valid only when the fluctuation levels are small compared to U . As a consequence, providing the restrictions on equation (9) are satisfied, a direct proportionality exists between frequency and wave-number.

Since velocity fluctuations were not measured in this investigation, an interpretation of the results on a wave-number basis is not appropriate.

Temperature spectra measured in mercury are shown in Fig. 11. The spectra appear to be

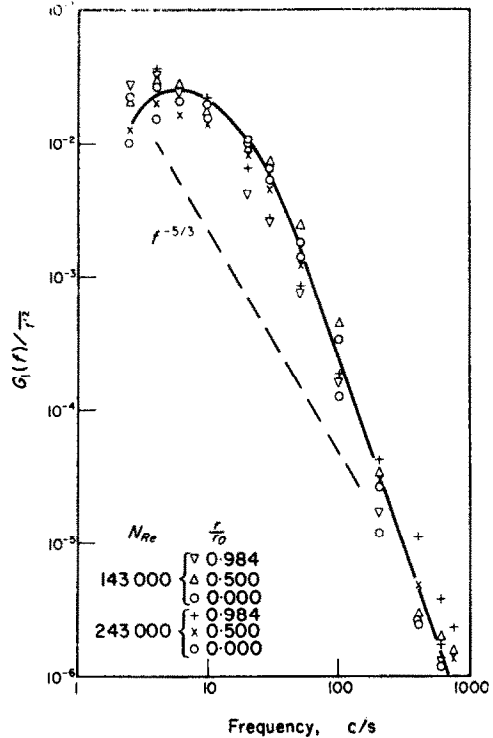


FIG. 11. Temperature spectra for mercury.

independent of position and Reynolds number although the scatter of the data masks possible second order dependency effects. The apparent trend of the data indicates some agreement with Corrsin's or Batchelor's spectral theory in the region of frequencies from 20 to 60 cps where a $f^{-5/3}$ frequency dependence may be applicable. The agreement is not conclusive, however, since the measurements were not sufficiently accurate to define the dependency.

At frequencies above 60 cps, the temperature spectra show the dependence,

$$G(f) \sim f^{-3}.$$

This is not in agreement with Batchelor's prediction of a $f^{-17/3}$ dependence for the inertial-diffusive subrange, perhaps as a result of failure to satisfy the requirements of Kolmogoroff's universal equilibrium theory. Because of the high Reynolds numbers, "local" isotropy may exist in the velocity field; however, because of the appreciable temperature gradients throughout

the majority of the flow region, a production of temperature "energy" may occur within the inertial subrange. Another factor is that the probe (0.015 in diameter) may be too large for measuring the properties of the small-scale temperature fluctuations.

Because of the uncertainties regarding the flow fields and the probe's capability of making accurate spectrum measurements, the spectrum data should be interpreted with caution. Certainly these data should not be used as a basis for validating Batchelor's spectral theory.

Figure 12 illustrates temperature spectra measured in ethylene glycol at a Reynolds number of 12 600. Within a frequency range of 20–60 cps, there is apparent agreement with Corrsin's or Batchelor's $f^{-5/3}$ dependence for the temperature spectrum. At higher frequencies the spectrum is dependent upon the relative locations within the flow channel. For frequencies above 100 cps, the temperature spectrum at the wall shows a dependence,

$$G(f) \sim f^{-2.5},$$

and at a distance from the wall ($|r/r_0| < 0.75$) the temperature spectra follows the relation

$$G(f) \sim f^{-2.0}.$$

There is some evidence of inverse square turbulence decay behind a grid in water-channel experiments reported by Tan and Ling [19].

Although the spectral data provide a preliminary indication of the structure of turbulent pipe flow, it is appropriate to delay careful analysis until additional information becomes available. It is difficult, for example, to assess agreement, or lack of it, with Batchelor's spectral theory until further work on the present system providing information regarding the velocity field becomes available. A study of the effect of probe size is also pertinent.

Amplitude distribution

The amplitude distribution of the temperature fluctuations may be described by the first probability density function, $P(x)$. Figure 13 illustrates typical values of $P(x)$, for mercury and ethylene glycol, normalized to a r.m.s. temperature or standard deviation of unity. For purposes of comparison, $P(x)$ for a Gaussian distributed random variable is also shown in

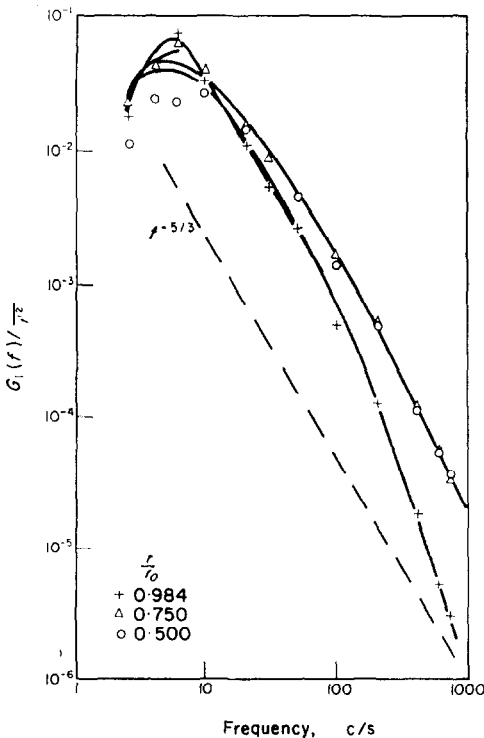


FIG. 12. Temperature spectra for ethylene glycol at N_{Re} equal to 12 600.

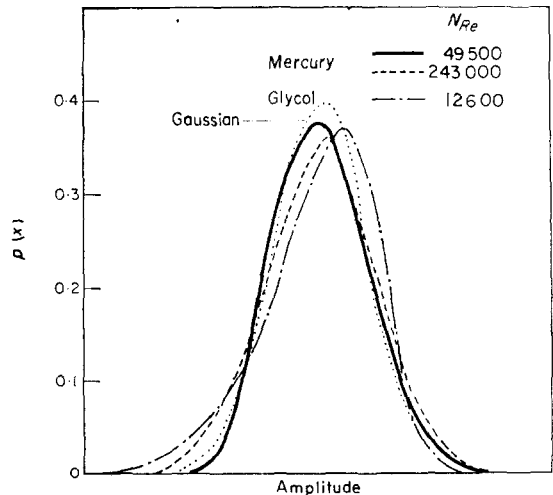


FIG. 13. Probability density function of t' in mercury and ethylene glycol.

Fig. 13; and, as shown, the temperature fluctuations for the examples are not Gaussian distributed.

As an easier means of showing trends in amplitude distribution with Reynolds number and spatial position, the data are presented in terms of the cumulative probability distribution function which is defined by

$$P(X) = \int_{-\infty}^x P(x) dx \quad (10)$$

When plotted on probability paper, cumulative probability distribution functions show straight-line representations for Gaussian distributed variations. Consequently, the departure of measured values of $P(X)$ from a straight-line representation is a measure of the deviation of the temperature fluctuations from a Gaussian distribution.

Figure 14 illustrates probability distribution functions of mercury and ethylene glycol temperature fluctuations at different positions and Reynolds numbers. The ordinates are in arbitrary units.

The curved-line representations of $P(X)$ in Fig. 14 show that the temperature fluctuations in mercury are not Gaussian distributed in a

range of Reynolds number from 49 500 to 243 000. There is no definite trend to show a dependence of $P(X)$ on position or Reynolds number.

For temperature fluctuations in ethylene glycol, the probability distribution functions are dependent upon position and Reynolds number. At a Reynolds number of 12 600, $P(X)$ is represented by a curved-line in the vicinity of the wall. In the interior region of the flow field, however, $P(X)$ is given by a straight-line which indicates the temperature fluctuations are Gaussian distributed. The probability distribution functions at a Reynolds number of 5800 are not Gaussian, although there is a tendency toward a Gaussian distribution in the interior flow region.

Corrsin [20] reported that the skewness of velocity probability density functions is dependent upon local gradients of the velocity intensity. An analogous dependence is shown by the probability density functions of temperature fluctuations. In the flow regions in ethylene glycol which display Gaussian distributed temperature fluctuations, the local r.m.s.-temperature gradients are small. In the region near the wall in ethylene glycol and throughout the majority of the flow field in mercury, the r.m.s.-temperature gradients are appreciable and the probability density functions of the temperature fluctuations are skewed.

The results of the amplitude and spectrum measurements show that isotropic temperature fluctuations appear to exist in ethylene glycol at low Reynolds numbers and not exist in mercury at high Reynolds numbers. On the basis of these results, it appears that the Reynolds number is not a useful flow dependent parameter which determines the "microscopic" properties of the temperature field. The Péclet number, on the other hand, may serve to determine the conditions necessary to achieve isotropy in the temperature field. In the measurements that were taken, the Péclet numbers ranged from 2.5×10^5 to 5×10^5 in ethylene glycol and from 800 to 4000 in mercury. Consequently, large Péclet numbers appear to be necessary to have isotropy in the temperature field. However, this preliminary conclusion needs more experimental justification.

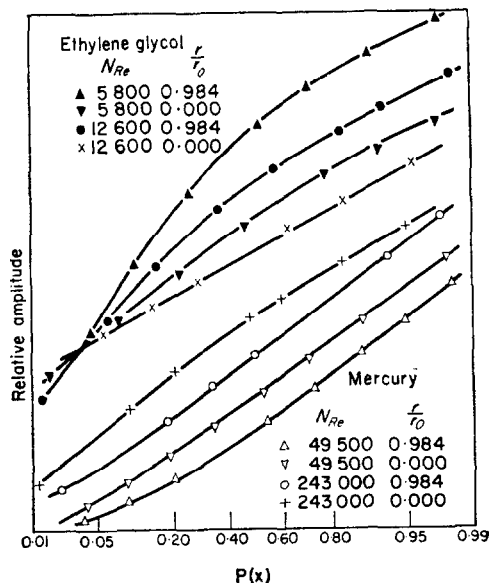


FIG. 14. Probability distribution function of t' mercury and ethylene glycol.

ACKNOWLEDGEMENT

The authors are grateful to the National Science Foundation for the financial support that made the research possible.

REFERENCES

1. O. E. DWYER and R. N. LYON, Liquid metal heat transfer, *Proceedings of the 3rd Geneva Conference on the Peaceful Uses of Atomic Energy*, P/225 (1964).
2. S. CORRSIN, The decay of isotropic temperature fluctuations in an isotropic turbulence, *J. Aeronaut. Sci.* **18**, 417 (1951).
3. S. CORRSIN, On the spectrum of isotropic temperature fluctuations in an isotropic turbulence, *J. Appl. Phys.* **22**, 469-473 (1951).
4. G. K. BATCHELOR, Small scale variations of convected quantities like temperature in turbulent fluid, Part 1, *J. Fluid Mech.* **5**, 113-133 (1959).
5. G. K. BATCHELOR, I. D. HOWELLS and A. A. TOWNSEND, Small scale variations of convected quantities like temperature in turbulent fluid, Part 2, *J. Fluid Mech.* **5**, 134-139 (1959).
6. S. CORRSIN, Further generalization of Onsager's cascade model for turbulent spectra, *Physics Fluids* **7**, 1156-1159 (1964).
7. A. L. KROTTER, V. O'BRIEN and S. CORRSIN, Preliminary measurements of turbulence and temperature fluctuations behind a heated grid, *NACA Res. Memo.* 54D19 (1954).
8. S. CORRSIN *et al.*, Turbulence and temperature fluctuations behind a heated grid, *NACA Tech. Note* 4288 (1958).
9. V. I. SUBBOTIN, M. K. IBRAGIMOV and M. N. IVANOVKII, Turbulent temperature pulsations in a liquid stream, *Atomnaya Energiya* **8**, (3) 254-257 (1960).
10. V. I. SUBBOTIN, M. K. IBRAGIMOV and E. V. NOMOFILOV, Measurement of turbulent temperature pulsations in liquid flow, *Teploenergetika*, No. 3, 64-67 (1962).
11. D. S. JOHNSON, Velocity and temperature measurements in a turbulent boundary layer downstream of a stepwise discontinuity in wall temperature, *J. Appl. Mech.* **81**, 325-336 (1959).
12. S. TANIMOTO and T. J. HANRATTY, Fluid temperature fluctuations accompanying turbulent heat transfer in a pipe, *Chem. Engng Sci.* **18**, 307 (1963).
13. A. RODRIGUEZ-RAMIREZ, Characteristics of turbulent temperature fluctuations in air, M.S. Thesis, Purdue University, Lafayette, Indiana (1965).
14. C. A. SLEICHER and M. TRIBUS, Heat transfer in a pipe with turbulent flow and arbitrary wall-temperature distribution, *Trans. Am. Soc. Mech. Engrs* **78**, 789-796 (1956).
15. J. H. RUST, Characteristics of turbulent temperature fluctuations in mercury and ethylene glycol, Ph.D. Thesis, Purdue University (1956).
16. E. H. BUYCO, Heat and momentum transfer in liquid metals, Ph.D. Thesis, Purdue University (1961).
17. S. L. SCHROCK, Eddy diffusivities in Na-K alloy, Ph.D. Thesis, Purdue University (1964).
18. C. H. GIBSON and W. H. SCHWARZ, The universal equilibrium spectra of turbulent velocity and scalar fields, *J. Fluid Mech.* **16**, 365-384 (1963).
19. H. S. TAN and S. C. LING, On the final stage decay of grid produced turbulence, Report TAR-TR 636, THERM. Inc. Ithaca, New York (1963).
20. S. CORRSIN, Hypothesis for skewness of the probability density of the lateral velocity fluctuations in turbulent shear flow, *J. Aeronaut. Sci.* **17**, 396-398 (1950).
21. J. NIKURADSE, Gesetzmässigkeit der turbulenten Strömung in glatten Röhren, *Forschift. Ver. Dt. Ing.* 356 (1932).

Résumé—Les fluctuations turbulentes de température dans le mercure et l'éthylène glycol ont été mesurées avec un thermocouple à réponse rapide ayant une constante de temps de l'ordre de 10^{-4} s. Des explorations transversales ont été faites à travers une section d'essais horizontale de 23,5 mm de diamètre ayant une température pariétale uniforme.

Les caractéristiques des fluctuations de température mesurées comprennent la valeur de la racine carrée de la moyenne quadratique, la distribution de l'amplitude et la distribution de fréquence, en fonction, dans chaque cas, de la position dans l'espace et du nombre de Reynolds.

On a trouvé que la distribution d'amplitude n'est pas gaussienne avec une déviation plus grande pour le mercure. L'énergie moyenne des fluctuations est à des fréquences de l'ordre 8 à 23 Hz.

Les longueurs de mélange thermique concorde assez bien avec les longueurs de mélange théoriques de von Kármán. Les résultats de densité spectrale suivent seulement d'une manière partielle la loi de Corrsin, en fonction de la fréquence.

Zusammenfassung—Mit einem schnell ansprechenden Thermoelement mit einer Zeitkonstanten von der Grössenordnung 10^{-4} s wurden turbulente Temperaturschwankungen in Quecksilber und Äthylenglykol gemessen. Quermessungen wurden durchgeführt in einer horizontalen Messtrecke von 23,5 mm Durchmesser bei gleichmässiger Wandtemperatur.

Charakteristika der gemessenen Temperaturschwankungen erstreckten sich auf die Wurzel des quadratischen Mittelwerts und die Amplituden- und Frequenzverteilung als Funktion der räumlichen Lage und der Reynoldszahl.

Die Amplitudenverteilung folgte nicht der Gaussfunktion und besass in Quecksilber eine grössere Abweichung. Die mittlere Schwankungsenergie liegt bei Frequenzen um 8–23 Schwingungen pro Sekunde. Die thermischen Mischlängen lassen sich verhältnismässig gut mit den theoretischen Mischlängen nach von Kármán vergleichen. Die spektralen Dichteergebnisse folgen nur teilweise der Corrsin'schen Frequenzabhängigkeit.

Аннотация—Турбулентные температурные флуктуации в ртути и этилен-гликоле измерялись с помощью быстро срабатывающей термопары, имеющей временную константу порядка 10^{-4} сек. Перемещение проводилось по горизонтальному поперечному сечению диаметром 0,925 дюйма при однородной температуре стенки.

Измеренные характеристики температурных флуктуаций включают среднеквадратичное значение и амплитудные и частотные распределения в каждом случае как функции положения в пространстве и числа Рейнольдса.

Найдено, что распределение амплитуды является не гауссовым с большим отклонением в ртути. Средняя энергия флуктуаций находится при частотах порядка 8–23 об/сек.

Тепловая длина смещения допускает хорошее сопоставление с теоретической длиной смещения Кармана.

Результаты для спектральных плотностей только частично следуют частотной зависимости Коррзина.